Evaluation of Laser Bacterial Anti-Fouling of Transparent Nanocrystalline Yttria-Stabilized-Zirconia Cranial Implant

Yasaman Damestani, PhD,[1] Natalie De Howitt, BS,[1] David L. Halaney, BS,[2] Javier E. Garay, PhD,[3] and Guillermo Aguilar, PhD[1,2]*

[1]*Department of Bioengineering, University of California – Riverside, Riverside, California 92521*
[2]*Department of Mechanical Engineering, University of California – Riverside, Riverside, California 92521*
[3]*Department of Mechanical and Aerospace Engineering, University of California – San Diego, La Jolla, California 92093*

Background and Objective: The development and feasibility of a novel nanocrystalline yttria-stabilized-zirconia (nc-YSZ) cranial implant has been recently established. The purpose of what we now call "window to the brain (WttB)" implant (or platform), is to improve patient care by providing a technique for delivery and/or collection of light into/from the brain, on demand, over large areas, and on a chronically recurring basis without the need for repeated craniotomies. WttB holds the transformative potential for enhancing light-based diagnosis and treatment of a wide variety of brain pathologies including cerebral edema, traumatic brain injury, stroke, glioma, and neurodegenerative diseases. However, bacterial adhesion to the cranial implant is the leading factor for biofilm formation (fouling), infection, and treatment failure. *Escherichia coli* (*E. coli*), in particular, is the most common isolate in gram-negative bacillary meningitis after cranial surgery or trauma. The transparency of our WttB implant may provide a unique opportunity for non-invasive treatment of bacterial infection under the implant using medical lasers.

Study Design/Materials and Methods: A drop of a diluted overnight culture of BL21-293 *E. coli* expressing luciferase was seeded between the nc-YSZ implant and the agar plate. This was followed by immediate irradiation with selected laser. After each laser treatment the nc-YSZ was removed, and cultures were incubated for 24 hours at 37 °C. The study examined continuous wave (CW) and pulsed wave (PW) modes of near-infrared (NIR) 810 nm laser wavelength with a power output ranging from 1 to 3 W. During irradiation, the temperature distribution of nc-YSZ surface was monitored using an infrared thermal camera. Relative luminescence unit (RLU) was used to evaluate the viability of bacteria after the NIR laser treatment.

Results: Analysis of RLU suggests that the viability of *E. coli* biofilm formation was reduced with NIR laser treatment when compared to the control group ($P < 0.01$) and loss of viability depends on both laser fluence and operation mode (CW or PW). The results demonstrate that while CW laser reduces the biofilm formation more than PW laser with the same power, the higher surface temperature of the implant generated by CW laser limits its medical efficacy. In contrast, with the right parameters, PW laser produces a more moderate photothermal effect which can be equally effective at controlling bacterial growth.

Conclusions: Our results show that *E. coli* biofilm formation across the thickness of the nc-YSZ implant can be disrupted using NIR laser treatment. The results of this *in vitro* study suggest that using nc-YSZ as a cranial implant *in vivo* may also allow for locally selective, non-invasive, chronic treatment of bacterial layers (fouling) that might form under cranial implants, without causing adverse thermal damage to the underlying host tissue when appropriate laser parameters are used. Lasers Surg. Med. 48:782–789, 2016. © 2016 Wiley Periodicals, Inc.

Key words: windows to the brain; transparent cranial implant; biofilm laser therapy; bioluminescent bacteria; fouling control

INTRODUCTION

The fundamental aim of the window to the brain (WttB) implant/platform is to improve patient care by providing a technique for delivery and/or collection of light into/from the brain, on demand, over large areas, and on a chronically recurring basis without the need for repeated craniotomies. Transparent nanocrystalline yttria-stabilized-zirconia (nc-YSZ) provides both the transparency and toughness required for enhancing the light-based diagnosis and treatment of a wide variety of brain pathologies including cerebral edema, traumatic brain injury, stroke, glioma, and neurodegenerative diseases, among many others. Using optical coherence tomography

Conflicts of Interest Disclosures: All authors have completed and submitted the ICMJE Form for Disclosure of Potential Conflicts of Interest and none were reported.

Contract grant sponsor: National Science Foundation (NSF); Contract grant number: 1547014; Contract grant sponsor: UC-MEXUS Dissertation Research Grant; Contract grant sponsor: American Society for Lasers in Medicine and Surgery (ASLMS).

*Correspondence to: Guillermo Aguilar, PhD, Department of Mechanical Engineering, University of California – Riverside, Riverside, CA 92521. E-mail: gaguilar@engr.ucr.edu

Accepted 26 June 2016
Published online 8 July 2016 in Wiley Online Library (wileyonlinelibrary.com).
DOI 10.1002/lsm.22558

(OCT), we demonstrated the initial feasibility of nc-YSZ cranial implants within the context of cortical imaging of an acute murine model [1]. For optical clearing of the scalp temporarily, our study on delivery techniques of optical clearing agents (OCA) such as propylene glycol (PG) showed that the combination of heated PG, microneedling and vacuum pretreatments, and positive pressure post-treatment significantly enhanced the perfusion of this topically applied OCA [2].

Unfortunately, bacterial adhesion to cranial implant biomaterials (fouling) is followed by colonization, biofilm formation, infection and, eventually, implant failure [3]. Despite advances in sterilization and antiseptic techniques, deep infection is the major leading complication after cranioplasty, with reported rates between 21% and 40% [4–7]. Infection might evolve due to contamination during surgery, local infections elsewhere in the body, or suppressed immune system [8]. Thus, bacterial adhesion to the implant and biofilm formation may limit the use of WttB for optical imaging and therapy, especially in immunocompromised patients. In particular, *Escherichia coli* (*E. coli*) is one of the most common isolates in gram-negative bacillary meningitis after cranial surgery or trauma in adults [3,9]. It has also been shown that *E. coli* peritonitis causes increased blood-brain barrier permeability [10]. Due to poor penetration of antimicrobial agents to the cerebrospinal fluid and resistance of biofilms to antimicrobial agents, the conventional treatment for cranial implant infection is removal and replacement of the implant, adding delays and cost to cranioplasties [11,12].

Sterilization of implant surfaces using lasers has been suggested [13,14] and resulted in several promising reports [15,16]. Previous data, however, demonstrates that temperature increase of 10 °C induces tissue damage in the bone [17–19] and denaturation of lipids and proteins [20]. Therefore, it is critical to ensure that the temperature change stays below this threshold for thermal damage during laser application.

Genetically engineered bacteria that express luciferase, from the American firefly, has been used in several models to optically monitor bacterial number and viability in real time [21]. Bioluminescence occurs when luciferase catalyzes the formation of the luciferin excited state in the presence of Mg^{2+}, ATP, and oxygen. Therefore, light can only be produced from live and metabolically active cells, which are able to generate ATP [22]. Validation of a non-invasive, real-time imaging technology using bioluminescent *E. coli* has been demonstrated in the neutropenic mouse thigh model of infection [23]. This demonstration showed that the intensity of luminescence images is proportional to the magnitude of the infection.

The transparency of the nc-YSZ implant provides us with the unique opportunity to shine a near-infrared (NIR) laser to treat the infected biomaterial locally and chronically, on-demand, without the need for removing the implant. Although the use of lasers to reduce bacterial growth *in vitro* was previously reported [24–26], the use of a transparent nc-YSZ implant for a non-invasive laser treatment of implant fouling is entirely novel. The objective of this *in vitro* study was to model bacterial growth underneath the nc-YSZ implant (i.e., implant fouling) and study the efficacy of distinct NIR laser irradiation parameters to disrupt bacteria viability and biofilm formation. The results from this *in vitro* model provide a strategy to study properties of nc-YSZ transparent cranial implants prior to investigations in more complex models such as *in vivo* animal studies.

MATERIALS AND METHODS

Implant Fabrication and Preparation

Transparent nc-YSZ (8 mol.% of Yttria) cranial implants were fabricated with current activated pressure assisted densification (CAPAD), an emerging technique that enables reduction of internal porosity to nanometric dimensions, and thus, reduction of the optical scattering that renders typical YSZ opaque [27]. Details of nc-YSZ fabrication and optical characterization have been reported previously [28,29], and %Transmittance measured with a Varian Cary 500 spectrophotometer (350–3,300 nm) and Equinox 55 FTIR spectrometer (3,300–13,000 nm) is provided in Figure 1. The room temperature thermal conductivity (κ) for nc-YSZ has been reported previously as $\sim$2–2.45 $W\,m^{-1}\,K^{-1}$ [30], and the specific heat (C_p) of YSZ (an intrinsic material property which does not exhibit any significant dependence on stabilizer content, phase composition or microstructure) has been reported as $427 \pm 14\,J\,kg^{-1}\,K^{-1}$ [31]. The volumetric density (ρ) of the nc-YSZ samples used in this study was measured to be $6042\,kg\,m^{-3}$, allowing for the thermal diffusivity (α) of our samples to be calculated as $\sim 7.75 \times 10^{-3}$–$9.49 \times 10^{-3}\,cm^2\,s^{-1}$ (see footnote[1]). The nc-YSZ samples used in this study were circular discs of 19.07 mm diameter and 0.70 mm thickness, and the average surface roughness (Ra) was measured using atomic force microscopy (AIST-NT) to be approximately 10 nm. Prior to each experiment, nc-YSZ samples were dry sterilized (Germinator 500) at 250 °C for 10 seconds to remove all pre-existing bacteria.

Bacteria Inoculation

For all experiments, genetically engineered BL21 *E. coli* (CMC0014, Sigma–Aldrich, St. Louis, MO) phenotype that emits bioluminescence was used. Briefly, BL21 cells were transformed with *P. Pyralis* luciferase gene on pET28b(+) vector. The transformants were cultured in Lysogeny Broth (LB) media supplemented with Kanamycin antibiotic (K^+). Laser irradiation experiments were run on agar plates containing K^+ and protein expression inducer Isopropyl
β-D-1-thiogalactopyranoside (IPTG). Specifically, BL21 *E. coli* culture was grown overnight in a shaker at 37 °C for 16 hours in the LB-K^+ until the OD_{600} reached 0.6–0.7.

[1] $\alpha = \kappa/(\rho \cdot C_p)$ α = thermal diffusivity, κ = thermal conductivity = 2–2.45 $W\,m^{-1}\,K^{-1}$, ρ = density = 6042 $kg\,m^{-3}$, C_p = specific heat = 427 $J\,kg^{-1}\,K^{-1}$. $\alpha = (2\text{–}2.45\,W\,m^{-1}\,K^{-1})/(6{,}042\,kg\,m^{-3} \cdot 427\,J\,kg^{-1}\,K^{-1}) = 7.75 \times 10^{-3}$–$9.49 \times 10^{-3}\,cm^2\,s^{-1}$.

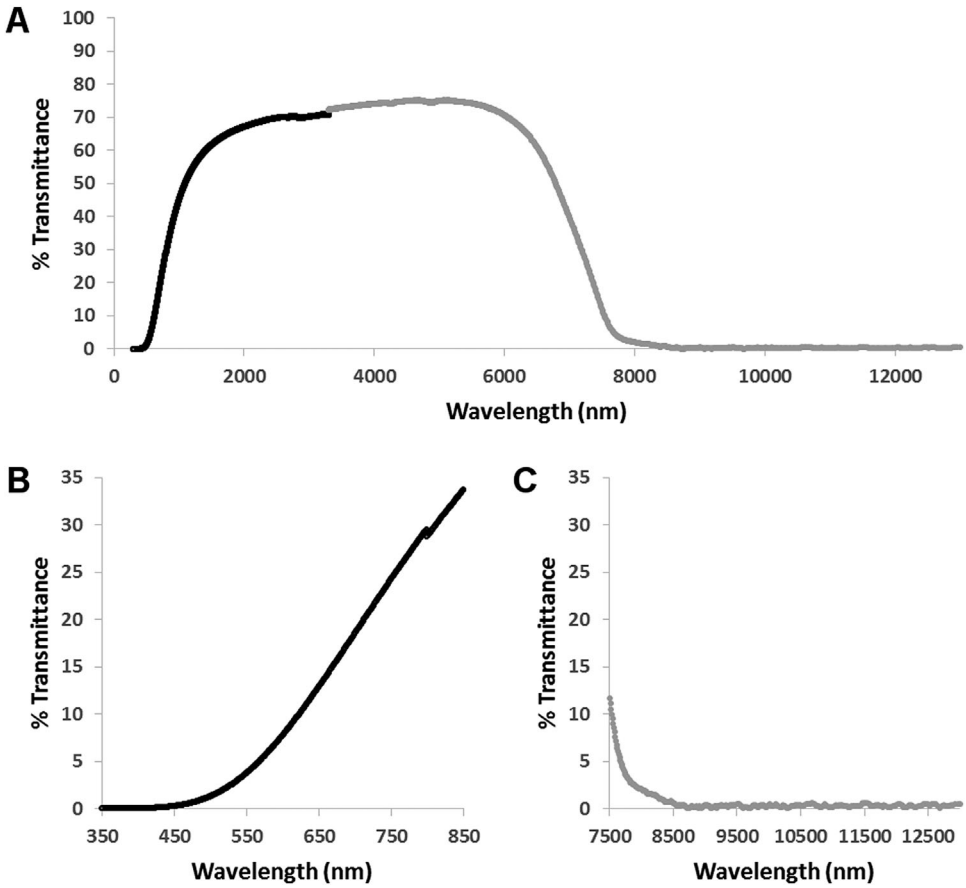

Fig. 1. (**A**) %Transmittance of nc-YSZ over the visible-IR spectral range. (**B**) Blowup of % Transmittance of nc-YSZ over the vis-NIR spectral range, including the laser treatment wavelength of 810 nm. (**C**) Blowup of %Transmittance of nc-YSZ over the IR spectral range measured by the infrared thermal camera. The black curve was measured with a Varian Cary 500 spectrophotometer (350–3,300 nm) and the gray curve was measured with an Equinox 55 FTIR spectrometer (3,300–13,000 nm).

One microliter of the overnight culture was diluted in 100 μL of fresh LB-K^+ media. As shown in Figure 2, agar plates were placed on a heated pad set to body-temperature in order to simulate *in vivo* conductivity and diffusivity of heat. For each experiment, 0.5 μL of the diluted bacteria was seeded on agar and the nc-YSZ was placed on top. The bacteria underlying nc-YSZ was treated with selected laser parameters through the nc-YSZ. The nc-YSZ was then removed from the culture and the plate was incubated for 24 hours at 37 °C.

Laser Device

Photo-irradiation was performed using an 810 nm laser (Vari-Lase) operated in continuous (CW) and pulse (PW) modes. The laser beam was coupled into a 600 μm optical

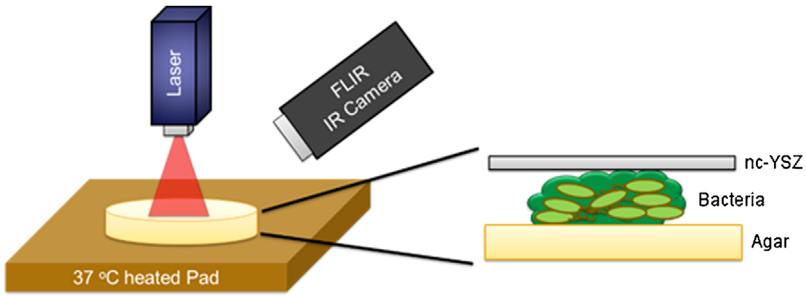

Fig. 2. Schematic diagram for the treatment of biofilm formation under nc-YSZ with NIR laser irradiation.

fiber to produce a 7 mm diameter ($1/e^2$) circular spot with a Gaussian profile on the nc-YSZ. The variable laser parameters were power (1–3 W corresponding to 2.6–7.8 W cm^{-2}) and pulse rate (0.3–5 Hz), and all laser treatments were 20 seconds in duration. Each combination of radiant exposure and frequency modulation was tested a total of nine times. Control cultures were treated in an identical manner to the irradiated cultures, except that the laser was not switched on.

Temperature Measurements

During laser treatment, the temperature of the surface of nc-YSZ was recorded with a non-contact infrared thermal camera (A325sc, FLIR Systems Inc., Wilsonville, OR) operating in video mode at 60 frames/s over the spectral range of 7.5–13 μm. Over this wavelength range, the nc-YSZ implant was essentially opaque (Fig. 1c), and thus the IR radiation measured by the camera was primarily emitted by the upper surface of the implant, and not originating from the underside of the implant in contact with the bacteria. The video was post-processed using ResearchIR software (FLIR ResearchIR4). According to specifications, the camera measures temperatures with a precision of 50 mK, has an accuracy of 2%, and a viewing angle of 5–60°.

Bioluminescence Imaging System

Following the 24 hours incubation, 100 μL of luciferin solution (13.4 μg of D-Luciferin potassium salt/mL; Research Products International Corp., Mt Prospect, IL) was added at room temperature to evenly cover each agar plate containing the irradiated bacteria (hereafter referred to as "sample") in preparation for bioluminescence measurements. Luciferin diffuses through the cell membrane where it reacts with the luciferase that is expressed by the *E. coli* to produce oxyluciferin. The decay of oxyluciferin produces a photon of light. Light emission of the bioluminescent bacteria was measured using a Macro Luminescence Dark Box (Stanford Photonics, Inc., Palo Alto, CA) in darkness with 5 seconds exposure at 2 MHz rate. ImageJ software (National Institute of Health) was used to quantify the light emission intensity at the irradiated Regions of Interest (ROIs). The ROIs encompassed a circle equal to the beam spot size on the sample (7 mm diameter). The relative luminescence unit (RLU) in the ROI was normalized with respect to the RLU outside of the ROI for each sample. The imaging procedure, acquisition parameters, and post-analysis were kept constant for all measurements.

Statistical Analysis

The difference between normalized RLU of control samples and laser-irradiated samples was statistically evaluated using analysis of variance for repeated measurements (ANOVA). When appropriate, *post hoc* analyses were performed with the Bonferroni's multiple comparisons test. Thompson Tau test was used to remove outliers. All statistics were calculated using GraphPad Prism 5.01 (GraphPad Software, Inc., San Diego, CA). Changes were considered statistically significant when the *P*-value was less than 0.05.

RESULTS

Figure 3 shows normalized RLU of biofilm after 24 hours and the average temperature (ΔT) of the upper surface of the nc-YSZ at the end of the 20 seconds laser treatment using CW laser with 1, 2, and 3 W of power and 20 seconds of exposure time to deliver a total of 20, 40, 60 J of energy, respectively. The results show that the decrease in the RLU value is statistically significant for all treated groups compared to control ($P < 0.05$) and that ΔT for the CW laser powers above 1 W is above 10 °C, which is considered the critical threshold for thermal damage. When CW laser is used, the reduction in biofilm formation seems to follow a linear relationship with ΔT.

Figure 4 shows normalized relative luminescence unit (RLU) of biofilm after 24 hours and the average temperature (ΔT) of the upper surface of the nc-YSZ at the end of the 20 seconds laser treatment using CW or PW laser with 3 W of power. Treatment with all laser parameters except for 0.5 and 0.3 Hz leads to a significant reduction of *E. coli* viability compared to the control group ($P < 0.05$). The results indicate that the ΔT is above the 10 °C critical temperature threshold for CW laser and all the PW laser settings exceeding 200 ms pulse duration and 1 Hz, when 3 W power is used.

Comparing bar #3, bar #5, bar #6, and bar #7 (frequency of 5, 1, 0.5, and 0.3 Hz, respectively) in Figure 4 indicates that laser treatment with higher frequency results in greater reduction in *E. coli* biofilm formation. Comparing bar #4 and bar #5 (1 Hz 400 ms vs. 1 Hz 200 ms) indicates that doubling the energy density per pulse and pulse duration increases the temperature of the surface of the implant by about 3 °C while it has negligible effect on the reduction rate of *E. coli* biofilm formation.

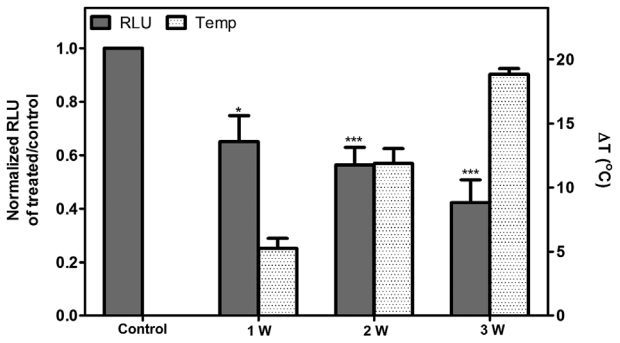

Fig. 3. Normalized relative luminescence unit (RLU) of biofilm after 24 hours and the average temperature (ΔT) of the upper surface of the nc-YSZ at the end of the 20 seconds laser treatment using CW laser with 1, 2, and 3 W of power to deliver a total of 20, 40, 60 J of energy, respectively. Each bar represents mean ± SEM ($n = 9$ for each treatment). One-way ANOVA and Bonferroni's multiple comparison test $^{*}P < 0.05$, $^{**}P < 0.01$, $^{***}P < 0.001$ relative to control.

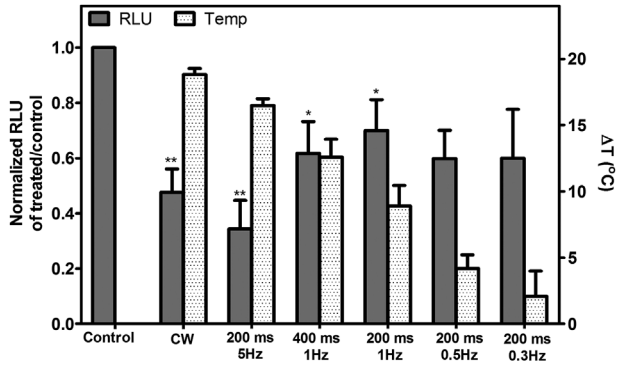

Fig. 4. Normalized relative luminescence unit (RLU) of biofilm after 24 hours and the average temperature (ΔT) of the upper surface of the nc-YSZ at the end of the 20 seconds laser treatment using 3 W of power with CW and PW modes. Each bar represents mean ± SEM ($n = 9$ for each treatment). One-way ANOVA and Bonferroni's multiple comparison test $^{*}P < 0.05$, $^{**}P < 0.01$, $^{***}P < 0.001$ relative to control.

The results indicate that CW laser has the higher reduction rate of *E. coli* biofilm formation compared to PW laser at the same power (3 W), but also causes a greater increase in temperature. In contrast to the linear relationship of temperature and reduction in biofilm formation for CW laser (Fig. 3), there is no linear relationship between the differences in temperature change and the distinct variability of the bactericidal effects of PW laser (Fig. 4).

DISCUSSION

WttB provides the transparency and toughness required for clinically viable cranial implants for optical therapy and imaging of the brain [1]. Zirconia surfaces have lower bacteria adhesion compared to other implant materials [32], however, infection due to implantitis is the most significant risk factor associated with cranial implants independent of the implant material [33]. In almost all cases of cranial implant infection, it is recommended to remove and later replace the implant to avoid intradural propagation of the infection and the severe consequent risk [11]. Therefore, new treatment techniques are demanded as infections associated with cranial implants lead to chronic complications [34].

In this study, we chose 810 nm as our wavelength to conduct the laser treatment of bacteria for several reasons. Various NIR diode lasers and Nd:YAG lasers are commonly and successfully used in endodontics for disinfection of almost all bacteria species. Diode lasers ($\lambda = 810$ nm) have been used to effectively reduce the viability of biofilm that adhered to zirconia dental implant surfaces. Stubinger et al. [35] studied the effect of diode ($\lambda = 810$ nm), CO_2 ($\lambda = 10{,}600$ nm), and Er:YAG laser ($\lambda = 2{,}940$ nm) on surface properties of yttria-stabilized tetragonal zirconia polycrystal (Y-TZP) implant surface using SEM, confocal 3D white light microscopy (CWLM), and energy-dispersive X-ray (EDX), and demonstrated that currently, diode lasers seem to be the only laser systems offering surface preservation and safety in the treatment of peri-implantitis with zirconia, while longer wavelengths did not. On the other hand, as shown in Figure 1b, the %Transmittance of our nc-YSZ implant decreases for wavelengths lower than 810 nm, and thus 810 nm allowed for a higher fluence to reach the bacteria through the implant, as well as surface preservation of the implant.

Nussbaum et al. [36] have investigated the effects of CW and frequency modulated 810 nm laser on the growth of *E. coli* and other bacterial species in culture previously, and found that the effect is dependent upon several factors, including bacterial species, modulation frequency, irradiance, and radiant exposure. Interestingly, both promotion and inhibition of bacterial growth rates were achieved by modulation of the laser parameters. While CW laser promoted *E. coli* growth regardless of radiant exposure (up to 50 J cm^{-2}, with 0.015 W cm^{-2} irradiance), PW caused promotion and inhibition, depending on frequency and radiant exposure, but the trend was less clear. In a follow up study using CW 810 nm laser, Nussbaum et al. [37] found promotion of *E. coli* growth similar to their previous study, but also inhibition of *E. coli* growth when irradiance was doubled (0.03 W cm^{-2}) and radiant exposure was sufficiently high (>30 J cm^{-2}). In our study, we observed inhibited *E. coli* growth for all laser parameters investigated. It should be noted, however, that while the radiant exposures reached in our study were similar to those reached by Nussbaum et al., the irradiance used in our study was substantially higher.

Our study further differs from these previous works due to the presence of the nc-YSZ implant overlying the bacteria during the laser treatment. As shown in Figure 1b, the %Transmittance of the implant at 810 nm is ~30%, and thus only 30% of photons reach the *E. coli*. The remainder of the photons do not pass through the implant, and are primarily absorbed resulting in heating of the implant. Thus the observed reduction in biofilm formation may be due to direct (optical transmission through implant) or indirect (heating of implant) effects of the laser on the *E. coli*, or a combination of both direct and indirect effects.

To investigate these two simultaneous effects individually, we conducted an additional experiment where a 4 mm air gap was introduced between the bacteria and the implant during laser treatment. This air gap served as a thermal barrier to remove the indirect heating component, and isolate the direct optical effect on the bacterial growth. When the thermal component was removed, the statistically significant reduction in RLU of the biofilm is lost (Fig. 5). While both laser treatments (CW, 3 W and 5 Hz, 3 W, 200 ms, bar #2 and bar #3, respectively) caused an increase in normalized RLU relative to control, this increase was not statistically significant ($P = 0.4868$). This result demonstrates that the direct optical effect of the laser on the *E. coli*, alone, cannot account for the decrease in bacterial growth rate displayed in Figures 3 and 4.

Regarding the indirect effect of laser on the *E. coli* (i.e., heating of the implant), differences in the heat distribution

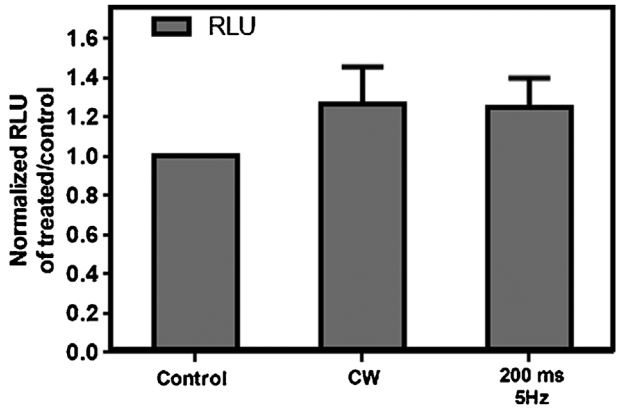

Fig. 5. Normalized relative luminescence unit (RLU) of biofilm 24 hours after 20 seconds laser treatment using 3 W of power with CW and PW modes, with 4 mm air gap between nc-YSZ and *E. coli*. Each bar represents mean ± SEM ($n = 3$ for each treatment). One-way ANOVA and Bonferroni's multiple comparison test $^{*}P < 0.05$, $^{**}P < 0.01$, $^{***}P < 0.001$ relative to control.

of the implant must be considered. As shown in Figure 1c, the implant is essentially opaque in the wavelength range measured by the thermal camera. Therefore, the temperatures reported in Figures 3 and 4 are only the temperature of the upper surface of the implant. Due to our experimental design, with the implant in physical contact with the bacteria during laser treatment (Fig. 2), it was not possible to measure the temperature of the lower surface of the implant during the treatments. To estimate this temperature, we repeated the laser treatments on the implant in isolation in air, and measured the ΔT of both the upper and lower surfaces of the implant. We then adjusted the ΔT of the upper surface of the implant reported in Figures 3 and 4 by this ratio (Table 1). Laser treatments of the agar plate in isolation resulted in negligible temperature increase of the agar (data not shown), and thus the estimated temperature of the lower surface of the implant shown in Table 1 can be treated as an approximate temperature experienced by the *E. coli* in the laser treatments from Figures 3 and 4.

Although there have been several *in vivo* and *in vitro* reports demonstrating the bactericidal effect of medical lasers on various strains, the underlying mechanisms of photochemical or/and photothermal effects remain controversial. Lee and Kaletunç [38] demonstrated that heating of *E. coli* from 55 to 70 °C for 60 seconds decreases the viability significantly due to enthalpy change and irreversible damage to ribosomal subunits. Using the temperature range of 50–70 °C and comparing temperature increase by CW high-power NIR laser (18–81 W cm^{-2}) and water bath, Hibst et al. [39] showed that inactivation of *E. coli* suspension is mainly driven by a thermal process. However, the estimated temperatures reached by the *E. coli* in our study (see Table 1) is much lower than the temperatures in these reports, and thus it is unlikely that the heating of the implant alone is responsible for the decrease in bacterial growth rate displayed in Figures 3 and 4.

As neither a direct optical effect (Fig. 5), nor an indirect thermal effect (Table 1) with the fluences and estimated temperatures reached in our study are alone sufficient to explain the observed inhibition in *E. coli* growth rate, it is possible that the combination of these effects is responsible. Lubart et al. [40] has previously suggested reactive oxygen species (ROS) generation as a mechanism for phototoxic effect of NIR light, while Nandakumar et al. [41] have reported that the bactericidal effect of laser is due to a reduction in ATP production which could in turn be due to damage of bacterial metabolic processes such as cellular respiration. While our results in Figure 5 showed that the isolated direct optical effect of the laser used in our study did not cause inhibition of the *E. coli* growth rate, perhaps the increased temperature of the *E. coli*, due to the indirect effect of the laser heating the implant, increases the susceptibility of the bacteria to these optical damage mechanisms. This possible explanation is speculative, and will require further study to determine the effect of *E. coli* temperature on the effectiveness of optical bactericidal treatments.

Further studies are essential to realize the potential of using lasers to reduce the formation of bacterial biofilm under the WttB *in vivo* due to differences in geometry, and optical and thermal properties of an *in vivo* model in comparison with the *in vitro* model used in this study. For example, one of the differences of an *in vivo* model is that the bacterial biofilm will have lower local temperatures than our *in vitro* model, due to the presence of corticospinal

TABLE 1. Estimated ΔT (°C) of the Lower Surface of the Implant at the End of the 20-Second Laser Treatments

	Measured ΔT (°C) of upper surface of implant	Measured ratio of ΔT (°C) of upper surface to ΔT (°C) of lower surface of implant	Estimated ΔT (°C) of lower surface of implant
CW, 1 W	5.27	2.88	1.83
CW, 2 W	11.79	2.69	4.38
CW, 3 W	18.85	2.64	7.14
5 Hz, 3 W, 200 ms	16.55	2.62	6.33
1 Hz, 3 W, 400 ms	12.62	2.74	4.60
1 Hz, 3 W, 200 ms	8.93	3.00	2.98
0.5 Hz, 3 W, 200 ms	4.17	3.11	1.34
0.3 Hz, 3 W, 200 ms	2.06	2.83	0.73

fluid (CSF) that can act as a thermal barrier to the brain. Moreover, the distance between the brain and the inner surface of the skull mapped by Fournier et al. [42] ranges from 0.4 to 6.7 mm. Therefore, depending on the actual location of the implant, this distance has to be considered in planning treatment. In addition, low-level laser therapy (LLLT) using 810 nm lasers has been shown to significantly improve the neurobehavioral performance of mice after closed head traumatic brain injury (TBI) [43]. Therefore, with careful choice of 810 nm laser parameters, treatment of biofilm formation can be performed along with LLLT treatment of TBI. Finally, although the estimated temperature reached by the bacteria underlying the implant is below the critical threshold of 10 °C, the temperature of the upper surface of the implant was unacceptably high for several of the laser parameters investigated in this study. Further studies will be needed to investigate methods of mitigating this high temperature during laser treatment, such as cryogenic cooling methods [44].

In conclusion, our results show that *E. coli* biofilm formation across the thickness of the nc-YSZ implant can be disrupted using NIR laser treatment. The results of this *in vitro* study suggest that using nc-YSZ as a cranial implant *in vivo* may also allow for local, non-invasive, chronic treatment of the formation of biofilm on the inner surface of the cranial implant, without inducing thermal damage to the underlying host tissue, when appropriate laser parameters are used. Further *in vivo* studies are necessary to investigate the efficacy of biofilm inhibition and lack of thermal damage to peri-implant tissue *in situ*.

ACKNOWLEDGMENTS

This study was supported, in part, by the National Science Foundation (NSF) award no. 1547014 to GA and JEG. The authors would like to acknowledge the UC-MEXUS Dissertation Research Grant awarded to YD to conduct this study. We would also like to thank the American Society for Lasers in Medicine and Surgery (ASLMS) for a travel grant awarded to YD to present research leading to this study at the 35rd Annual ASLMS Conference, Kissimmee, FL April 2015. Additionally, we thank Dr. Yasuhiro Kodera for providing the nc-YSZ samples.

REFERENCES

1. Damestani Y, Reynolds CL, Szu J, Hsu MS, Kodera Y, Binder DK, Park BH, Garay JE, Rao MP, Aguilar G. Transparent nanocrystalline yttria-stabilized-zirconia calvarium prosthesis. Nanomedicine 2013;9:1135–1138.
2. Damestani Y, Melakeberhan B, Rao MP, Aguilar G. Optical clearing agent perfusion enhancement *via* combination of microneedle poration, heating and pneumatic pressure. Lasers Surg Med 2014;46:488–498.
3. Briggs S, Ellis-Pegler R, Raymond N, Thomas M, Wilkinson L. Gram-negative bacillary meningitis after cranial surgery or trauma in adults. Scand J Infect Dis 2004;36:165–173.
4. Gordon CR, Fisher M, Liauw J, Lina I, Puvanesarajah V, Susarla S, Coon A, Lim M, Quinones-Hinojosa A, Weingart J, Colby G, Olivi A, Huang J. Multidisciplinary approach for improved outcomes in secondary cranial reconstruction: Introducing the pericranial-onlay cranioplasty technique. Neurosurgery 2014;10(Suppl 2):179–189; discussion 189–190.
5. Moreira-Gonzalez A, Jackson IT, Miyawaki T, Barakat K, DiNick V. Clinical outcome in cranioplasty: Critical review in long-term follow-up. J Craniofac Surg 2003;14:144–153.
6. Stephens FL, Mossop CM, Bell RS, Tigno T, Jr., Rosner MK, Kumar A, Moores LE, Armonda RA. Cranioplasty complications following wartime decompressive craniectomy. Neurosurg Focus 2010;28:E3.
7. Yadla S, Campbell PG, Chitale R, Maltenfort MG, Jabbour P, Sharan AD. Effect of early surgery, material, and method of flap preservation on cranioplasty infections: A systematic review. Neurosurgery 2011;68:1124–1129; discussion 1130.
8. Busscher HJ, Ploeg RJ, van der Mei HC. SnapShot: Biofilms and biomaterials; mechanisms of medical device related infections. Biomaterials 2009;30:4247–4248.
9. Wang KW, Chang WN, Huang CR, Tsai NW, Tsui HW, Wang HC, Su TM, Rau CS, Cheng BC, Chang CS, Chuang YC, Liliang PC, Tsai YD, Lu CH. Post-neurosurgical nosocomial bacterial meningitis in adults: Microbiology, clinical features, and outcomes. J Clin Neurosci 2005;12:647–650.
10. du Moulin GC, Paterson D, Hedley-Whyte J, Broitman SA. E. coli peritonitis and bacteremia cause increased blood-brain barrier permeability. Brain Res 1985;340:261–268.
11. Dashti SR, Baharvahdat H, Spetzler RF, Sauvageau E, Chang SW, Stiefel MF, Park MS, Bambakidis NC. Operative intracranial infection following craniotomy. Neurosurg Focus 2008;24:E10.
12. Goh RC, Chang CN, Lin CL, Lo LJ. Customised fabricated implants after previous failed cranioplasty. J Plast Reconstr Aesthet Surg 2010;63:1479–1484.
13. Haas R, Dortbudak O, Mensdorff-Pouilly N, Mailath G. Elimination of bacteria on different implant surfaces through photosensitization and soft laser. An *in vitro* study. Clin Oral Implants Res 1997;8:249–254.
14. Mason ML. Using the laser for implant maintenance. Dentistry Today 1992;11:74–75.
15. Kato T, Kusakari H, Hoshino E. Bactericidal efficacy of carbon dioxide laser against bacteria-contaminated titanium implant and subsequent cellular adhesion to irradiated area. Lasers Surg Med 1998;23:299–309.
16. Block CM, Mayo JA, Evans GH. Effects of the Nd:YAG dental laser on plasma-sprayed and hydroxyapatite-coated titanium dental implants: Surface alteration and attempted sterilization. Int J Oral Maxillofac Implants 1992;7:441–449.
17. Eriksson AR, Albrektsson T. Temperature threshold levels for heat-induced bone tissue injury: A vital-microscopic study in the rabbit. J Prosthet Dent 1983;50:101–107.
18. Kreisler M, Al Haj H, d'Hoedt B. Temperature changes at the implant-bone interface during simulated surface decontamination with an Er:YAG laser. Int J Prosthodont 2002;15:582–587.
19. Geminiani A, Caton JG, Romanos GE. Temperature increase during CO(2) and Er:YAG irradiation on implant surfaces. Implant Dent 2011;20:379–382.
20. He X. Thermostability of biological systems: Fundamentals, challenges, and quantification. Open Biomed Eng J 2011;5: 47–73.
21. Contag CH, Contag PR, Mullins JI, Spilman SD, Stevenson DK, Benaron DA. Photonic detection of bacterial pathogens in living hosts. Mol Microbiol 1995;18:593–603.
22. Dinjaski N, Suri S, Valle J, Lehman SM, Lasa I, Prieto MA, Garcia AJ. Near-infrared fluorescence imaging as an alternative to bioluminescent bacteria to monitor biomaterial-associated infections. Acta Biomater 2014;10:2935–2944.
23. Hamblin MR, O'Donnell DA, Murthy N, Contag CH, Hasan T. Rapid control of wound infections by targeted photodynamic therapy monitored by *in vivo* bioluminescence imaging. Photochem Photobiol 2002;75:51–57.
24. Sennhenn-Kirchner S, Klaue S, Wolff N, Mergeryan H, von Zepelin MB, Jacobs HG. Decontamination of rough titanium surfaces with diode lasers: Microbiological findings on *in vivo* grown biofilms. Clin Oral Implants Res 2007;18:126–132.
25. Nussbaum EL, Lilge L, Mazzulli T. Effects of low-level laser therapy (LLLT) of 810nm upon *in vitro* growth of bacteria:

Relevance of irradiance and radiant exposure. J Clin Laser Med Surg 2003;21:283–290.
26. Kim S, Kim J, Lim W, Jeon S, Kim O, Koh JT, Kim CS, Choi H. In vitro bactericidal effects of 625, 525, and 425nm wavelength (red, green, and blue) light-emitting diode irradiation. Photomed Laser Surg 2013;31:554–562.
27. Garay JE. Current-activated, pressure-assisted densification of materials. Annu Rev Mater Res 2010;40:445–468.
28. Alaniz JE, Perez-Gutierrez FG, Aguilar G, Garay JE. Optical properties of transparent nanocrystalline yttria stabilized zirconia. Opt Mater 2009;32:62–68.
29. Kodera Y, Hardin CL, Garay JE. Transmitting, emitting and controlling light: Processing of transparent ceramics using current-activated pressure-assisted densification. Scripta Mater 2013;69:149–154.
30. Ghosh S, Teweldebrhan D, Morales JR, Garay JE, Balandin AA. Thermal properties of the optically transparent pore-free nanostructured yttria-stabilized zirconia. J Appl Phys 2009;106:113507.
31. Amaya C, Caicedo JC, Yáñez-Limón JM, Vargas RA, Zambrano G, Gómez ME, Prieto P. A non-destructive method for determination of thermal conductivity of YSZ coatings deposited on Si substrates. Mater Chem Phys 2012;136:917–924.
32. Hauser-Gerspach I, Stubinger S, Meyer J. Bactericidal effects of different laser systems on bacteria adhered to dental implant surfaces: An *in vitro* study comparing zirconia with titanium. Clin Oral Implants Res 2010;21: 277–283.
33. Cho YR, Gosain AK. Biomaterials in craniofacial reconstruction. Clinics Plast Surg 2004;31:377–385.
34. Darouiche RO. Antimicrobial approaches for preventing infections associated with surgical implants. Clin Infect Dis 2003;36:1284–1289.
35. Stübinger S, Homann F, Etter C, Miskiewicz M, Wieland M, Sader R. Effect of Er:YAG, CO(2) and diode laser irradiation on surface properties of zirconia endosseous dental implants. Lasers Surg Med 2008;40:223–228.
36. Nussbaum EL, Lilge L, Mazzulli T. Effects of 810nm laser irradiation on *in vitro* growth of bacteria: Comparison of continuous wave and frequency modulated light. Lasers Surg Med 2002;31:343–351.
37. Nussbaum EL, Lilge L, Mazzulli T. Effects of low-level laser therapy (LLLT) of 810nm upon *in vitro* growth of bacteria: Relevance of irradiance and radiant exposure. J Clin Laser Med Surg 2003;21:283–290.
38. Lee J, Kaletunç G. Evaluation of the heat inactivation of Escherichia coli and Lactobacillus plantarum by differential scanning calorimetry. Appl Environ Microbiol 2002;68: 5379–5386.
39. Hibst R, Graser R, Udart M, Stock K. Mechanism of high-power NIR laser bacteria inactivation. J Biophotonics 2010;3:296–303.
40. Lubart R, Lipovski A, Nitzan Y, Friedmann H. A possible mechanism for the bactericidal effect of visible light. Laser Ther 2011;20:17–22.
41. Nandakumar K, Obika H, Shinozaki T, Ooie T, Utsumi A, Yano T. Laser impact on bacterial ATP: Insights into the mechanism of laser-bacteria interactions. Biofouling 2003;19:109–114.
42. Fournier M, Combes B, Braga J, Roberts N, Prima S. Mapping the distance between the brain and the inner surface of the skull: Interest for the study of fossil endocasts. Am J Phys Anthropol 2011;144:137–138.
43. Ando T, Xuan W, Xu T, Dai T, Sharma SK, Kharkwal GB, Huang YY, Wu Q, Whalen MJ, Sato S, Obara M, Hamblin MR. Comparison of therapeutic effects between pulsed and continuous wave 810-nm wavelength laser irradiation for traumatic brain injury in mice. PLoS ONE 2011;6:e26212.
44. Majaron B, Svaasand LO, Aguilar G, Nelson JS. Intermittent cryogen spray cooling for optimal heat extraction during dermatologic laser treatment. Phys Med Biol 2002;47: 3275–3288.